MDPI

Development and Application of the Snow, Soil Water and Water Balance Model (SNOSWAB), an Online Model for Daily Estimation of Snowpack Processes, Soil Water Content and Soil Water Balance

Serban Danielescu [ID]

Fredericton Research and Development Centre, Agriculture and Agri-Food Canada and Environment and Climate Change Canada, 95 Innovation Rd., Fredericton, NB E3B 4Z7, Canada; serban.danielescu2@agr.gc.ca

Abstract: SNOSWAB (<u>Sno</u>w, <u>S</u>oil <u>Wa</u>ter and <u>Wa</u>ter <u>B</u>alance) is a unique online deterministic model built using tipping-bucket approaches that allows for the daily estimation of (i) snowpack processes; (ii) soil water content; and (iii) soil water budget. SNOSWAB is most suitable for modeling field-scale processes for vertically and horizontally homogeneous soils, and its applicability is not limited to specific climate zones or geographical areas. The model is freely available, and its streamlined online interface integrates powerful calibration, visualization and data export routines. In this study, SNOSWAB development and a conceptual model, as well as an example of its application using data collected during a 12-year (2008–2019) field study conducted at the Agriculture and Agri-Food Canada Harrington Experimental Farm (HEF) on Prince Edward Island (PEI), Canada, are presented. Input data consisting of daily air temperature, total precipitation, rainfall and evapotranspiration were used in conjunction with soil properties and daily soil water content, snowpack thickness, surface runoff and groundwater recharge to calibrate (2010–2014) and validate (2015–2019) the model. For both the calibration and validation simulations, the statistical indicators used for evaluating model performance indicated, in most cases, high model fitness (i.e., $R^2 > 0.5$, NRMSE < 50% and $-25\% <$ PBIAS $< 25\%$) for the various time intervals and parameters analyzed. SNOSWAB fills an existing gap in the online environment and, due to its ease of use, robustness and flexibility, shows promise to be adopted as an alternative for more complex, standalone models that might require extensive resources and expertise.

Keywords: hydrological modeling; snow modeling; soil water content; infiltration; surface runoff; drainage; soil water budget; water deficiency; online tools; open science

1. Introduction

Soil water content, defined as the amount of water contained within the soil, is of fundamental importance for many hydrological, biological and biochemical processes [1–4] and, hence, knowledge of soil water content is relevant to many disciplines, such as soil science, hydrology and hydrogeology, agriculture, ecology, forestry, and civil and water resource engineering. In temperate or colder climates and areas with higher elevation, an understanding of snow processes (e.g., snowpack thickness, snowmelt, etc.) is critical for properly assessing the soil water content and soil water budget dynamics; for example, these processes are critical for baseflow and runoff formation as well as for the transport of excess nutrients from agricultural fields, but are difficult to measure [5–8]. Soil water content is a key component of the soil water budget and, hence, it contributes to controlling, for example, plant growth [9,10], the availability of water for drainage [11,12] and groundwater recharge [13,14], as well as the transport of contaminants [15,16] and pathogens [17] in the subsurface. Soil water content can in many cases be difficult, time-consuming or expensive to measure [18–20]. Hence, a wide range of models aimed at simulating soil

water content and dynamics have been developed. Numerous in-depth reviews of these models are available elsewhere [20–28]. The various types of models available can have various degrees of complexity, ranging, for example, from simple models (e.g., capacity or tipping-bucket models) to numerical models (e.g., based on finite-difference or finite-element algorithms), deterministic models (i.e., unique results based on a set of parameter values) or a combination of the above. The latter models, while more accurate, are also more data- and process-intensive and might require parameters that are not readily available. In addition, soil water models range from models limited to the simulation of a reduced number of processes to models that are able to simulate the majority of soil water processes, including interdependent processes (e.g., snowmelt, surface runoff, sublimation) and the soil water budget.

Soil water models are generally available as software packages, either free or commercially licensed. Examples of popular software packages that integrate the modeling of soil water content, soil water budget and additional processes include HYDRUS [29], a model for simulating the movement of water, heat and solutes in porous media; SWAT [30], used for assessing soil erosion, non-point-source pollution and management in watersheds; DSSAT [31], a dynamic crop growth simulation model; SWAP [32], a model for the simulation of the transport of water, solutes and heat in unsaturated/saturated soils; SWB [33], a model designed for the estimation of groundwater recharge; STICS [34], a model for the simulation of crop growth as well as the soil water budget and nitrogen cycle; RZWQM [35], a model that simulates plant growth and the movement of water, nutrients and pesticides over, within and below the crop root zone; and CROPWAT [36], a model developed for the calculation of crop water requirements and irrigation requirements. These models generally require extensive input datasets, such as daily meteorological data, soil and crop properties and agricultural management details.

In the online environment, models that allow for the estimation of soil water content and soil water budget terms, including processes controlling soil water content (e.g., snowpack dynamics, surface runoff, etc.), using a simplified approach have not been identified. The several online soil-water-content-related tools that were identified are aimed at estimating water availability for plants or their irrigation requirements. Examples of these simplistic models include the Soil Water Tool [37], a tool for estimating soil water available for crops; the Free Online Irrigation Calculator [38], a tool for irrigation scheduling, and a series of irrigation calculators [39,40] for estimating irrigation requirements associated with various irrigation methods. These tools rely on overly simplified approaches and provide only seasonal or annual estimates. In addition, none of these tools have capabilities for validating the estimates, modifying graphical and tabular visualizations of the input and output datasets or data exporting.

A series of models with complex structures are currently available in the online environment. Examples of complex online models include the Water Balance Model Online [41], a scenario-comparison and decision-support tool for establishing performance targets for rainwater capture and runoff control in British Columbia, Canada; the CSF Water Deficit Calculator [42], a tool for estimating soil water content in the root zone and crop water deficit in the northeastern United States; and Cool Farm Tool Water [43], a tool for the estimation of crop water use and the main components of soil water balance. Depending on the model, these models can benefit from integration into GIS platforms, can be incorporated or linked with various databases (e.g., geodatabases, weather, etc.) and can include non-hydrological components (e.g., greenhouse gas emissions). These models might be restricted to certain geographical areas and might allow the estimation of soil water content or soil water balance terms only for longer time intervals (e.g., multi-annual averages). To the best of author's knowledge, these models do not provide built-in capabilities for assessing the validity of the model output.

In this paper, the development of the SNOSWAB (<u>Sno</u>w, <u>S</u>oil <u>Wa</u>ter and Water <u>B</u>alance; https://snoswab.hydrotools.tech/; accessed on 20 May 2024) model and its application using data collected during a 12-year study (2008–2019) conducted on Prince Edward

Island, Canada, are presented. SNOSWAB is a unique, freely accessible online tipping-bucket (or capacity) deterministic model that has been developed in response to the current gap relative to the availability of easy-to-use online science-based hydrology tools. Thus, SNOSWAB, which is most suitable for modeling field-scale processes for vertically and horizontally homogeneous soils, can be used for the estimation of the daily dynamics of snowpack processes, soil water content and soil water budget based on user-provided meteorological and calibration data. The model integrates extensive calibration routines, and the user-provided calibration data are not restricted to particular variables of the model. SNOSWAB can be applied to any location for which input data are available and can be used for evaluating various scenarios relevant to the above processes. The model can be used for various purposes, for example, to support studies aimed at understanding subsurface water storage (e.g., soil storage, groundwater recharge), crop water stress, local- or watershed-scale water balances, and the impacts of climate change on soil water content or soil water balance. SNOSWAB can also be used for generating data for more complex models that allow for user-provided timeseries, as well as for education and demonstration purposes, by using the built-in sample datasets.

2. Materials and Methods

2.1. SNOSWAB Development

SNOSWAB [44] was developed through a collaborative research effort between Agriculture and Agri-Food Canada (AAFC, Ottawa, ON, Canada) and Environment and Climate Change Canada (ECCC, Ottawa, ON, Canada), Canadian Rivers Institute (CRI, Fredericton, NB, Canada) and the University of New Brunswick (UNB, Fredericton, NB, Canada), in response to the efforts of the Canadian federal government to encourage easier and open access to science [45]. Its development is the result of larger AAFC- and ECCC-led research efforts aimed at evaluating the linkages between agricultural production systems and groundwater and surface water quantity and quality in Atlantic Canada. SNOSWAB was programmed in PHP 7.4., has cross-browser compatibility and unrestricted public access and does not require user registration or software installation. Since its launch in March 2023, SNOSWAB has had ~2300 unique visitors, with users accessing the model from many regions of the globe.

SNOSWAB is part of the Hydrology Tool Set (HTS; https://www.hydrotools.tech, accessed on 20 May 2024) [46], a suite of tools and models that can be used for advancing our understanding of various local- and watershed-scale hydrological processes. Other tools currently available in the HTS include SepHydro for estimating surface runoff and groundwater contributions to streamflow via hydrograph separation [47,48]; ETCalc for the estimation of potential, reference and actual evapotranspiration [48,49]; SWIB for assessing crop water stress (either as water deficit or excess), soil water balance and irrigation requirements and its impact on aquifer storage [50,51]; RECHARGE BUDDY for the estimation of groundwater recharge [52]; and SNOWFALL BUDDY for the estimation of the snowfall and rainfall components of total precipitation [53]. The development of all the tools included in the HTS was based on the following key principles: (i) they are free to use; (ii) they have a user-friendly interface, with streamlined and easy-to-follow procedures; (iii) they have minimal input data requirements; and (iv) they provide a choice of methods and customizable parameters.

2.2. SNOSWAB Workflow

SNOSWAB has a modular structure, with the following four modules available: (i) the HOME module, which contains background information, including methodological details and a user guide; (ii) the INPUT DATA module, which allows for either using the built-in sample data or uploading daily user data; (iii) the SNOW module, which provides access to coefficients and calibration settings for snowpack processes; and (iv) the WATER BALANCE module, which provides access to coefficients and calibration settings for the soil water content and soil water budget components of the model (Figure 1). The INPUT

DATA, SNOW and WATER BALANCE modules include options for displaying univariate statistics for various averaging or custom-length time intervals, and the SNOW and WATER BALANCE modules also include options for displaying bivariate statistics for assessing the fitness of the model output. Each of the modules, except for the HOME module, provides access to tools for visualizing and customizing graphics and tabular data as well as for exporting input, output and configuration data (i.e., configuration settings).
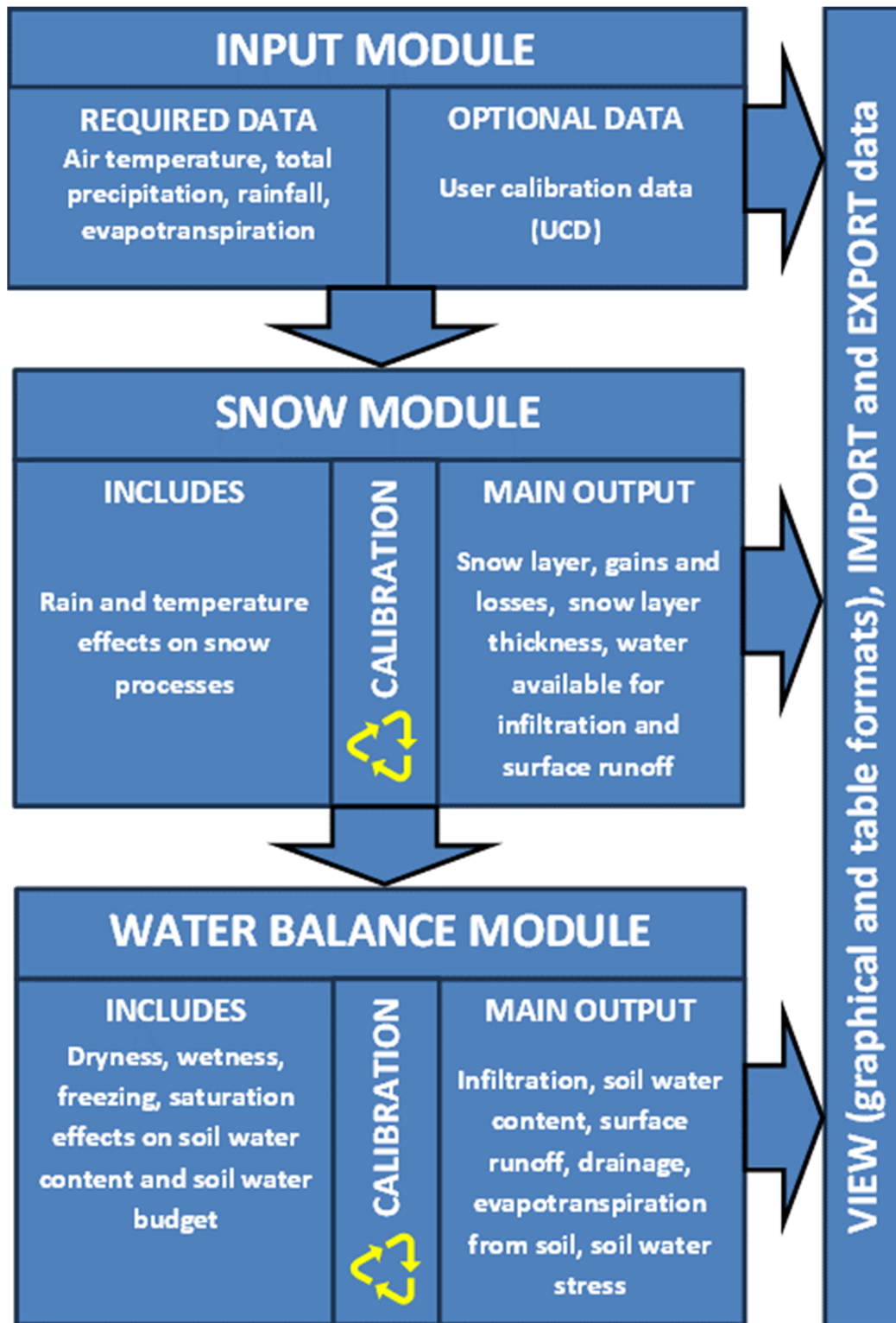

Figure 1. Simplified workflow diagram of the SNOSWAB model.

2.3. SNOSWAB Conceptual Model

In SNOSWAB, hydrological processes are separated into aboveground (i.e., SNOW module) and soil (WATER BALANCE module) processes. SNOSWAB calculations are conducted on a daily basis, and the output of the model is available on a daily basis as well as for various averaging time intervals.

The SNOW module integrates the snowpack-related processes and evapotranspiration (Figure 2). The main snowpack processes include net gain in the snowpack, net loss from the snowpack (i.e., net snowmelt) and snowpack accumulation (i.e., thickness of the snow layer). Snowpack accumulation is obtained by using a series of coefficients accounting for air temperature and precipitation as rain or snow (Table S1 in Supplementary Materials). Snowmelt, together with precipitation not accumulating into snowpack, becomes available for infiltration or surface runoff. Evapotranspiration is separated into aboveground and soil fractions. Aboveground evapotranspiration is attributed to processes such as canopy interception or water ponding. Evapotranspiration below the surface of the ground is representative of evaporative soil processes as well as plant transpiration. The amount of water available for infiltration or surface runoff and the soil fraction of evapotranspiration are transferred to the WATER BALANCE module for calculating soil water content and soil water budget terms. The equations governing the SNOW module calculations are included in Table S2 in the Supplementary Materials.
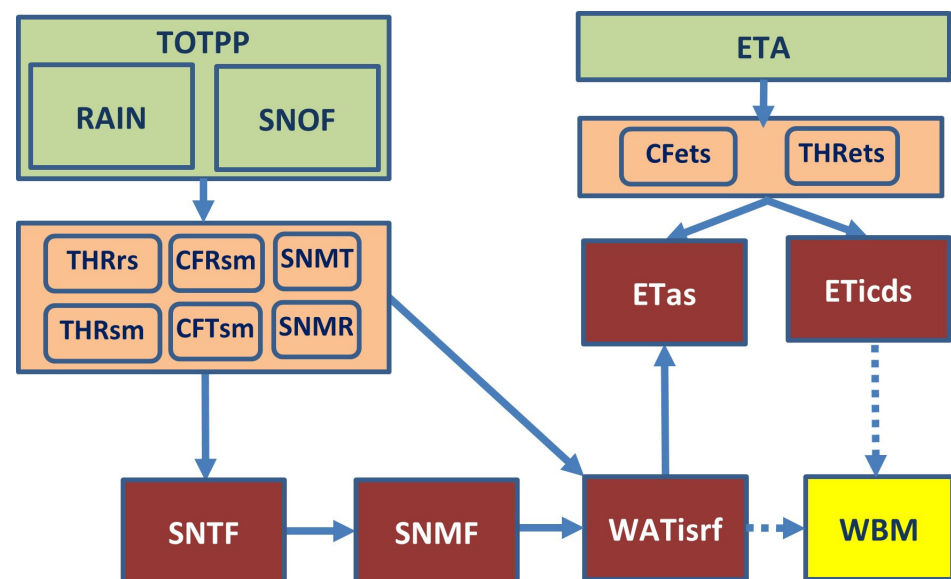

Figure 2. Simplified workflow diagram for the SNOSWAB SNOW module (green boxes—input data, orange boxes—module coefficients, red boxes—output variables, yellow box—connection with a different calculation module; TOTPP—daily total precipitation input data, ETA—daily actual evapotranspiration input data, RAIN—daily rain input data, SNOF—snowfall amount, CFets—correction factor for portion of evapotranspiration occurring in the soil, THRets—soil water content threshold for stopping soil evapotranspiration when the soil is dry, THRrs—air temperature threshold for rain to be accumulated as snow, CFRsm—correction factor for snowmelt due to rain, SNMT—snowmelt due to temperature, THRsm—air temperature threshold for initiating snowmelt, CFTsm—correction factor for snowmelt due to air temperature, SNMR—snowmelt due to rain, Etas—above-soil ET, ETicds—soil ET, SNTF—snow layer thickness, SNMF—[net] snowmelt, WATisrf—water available for infiltration or surface runoff; WBM—WATER BALANCE module; dashed lines indicate amounts transferred to WBM).

The WATER BALANCE module's main outputs are soil water content and soil water budget components (Figure 3). Soil water content is constrained by the amount of infiltration and drainage, which are controlled by the infiltration and drainage capacity of the soil. Drainage is further limited by soil evapotranspiration as well as dry and frozen soil conditions.

The amount of water that is not infiltrating becomes surface runoff. SNOSWAB also allows for direct transfers between surface runoff and drainage, without impacting soil water content. In addition, SNOSWAB includes routines for estimating the number of days with dry and wet soil conditions, to support studies related to crop water stress. For calculating the number of days with water stress for the case study included, the SWC was considered to be low when it was below 70% of the effective porosity, high when it was above 90% of the effective porosity and in the optimal range when it was between 80% and 90% of the effective porosity. The value of effective porosity was calculated using the maximum values of the SWC measured in the field, and the SWC thresholds were chosen based on a study conducted in the same field aimed at understanding the supplemental irrigation requirements for intensive potato cropping systems [50]. The equations governing the WATER BALANCE module calculations are included in Table S3 in the Supplementary Materials.
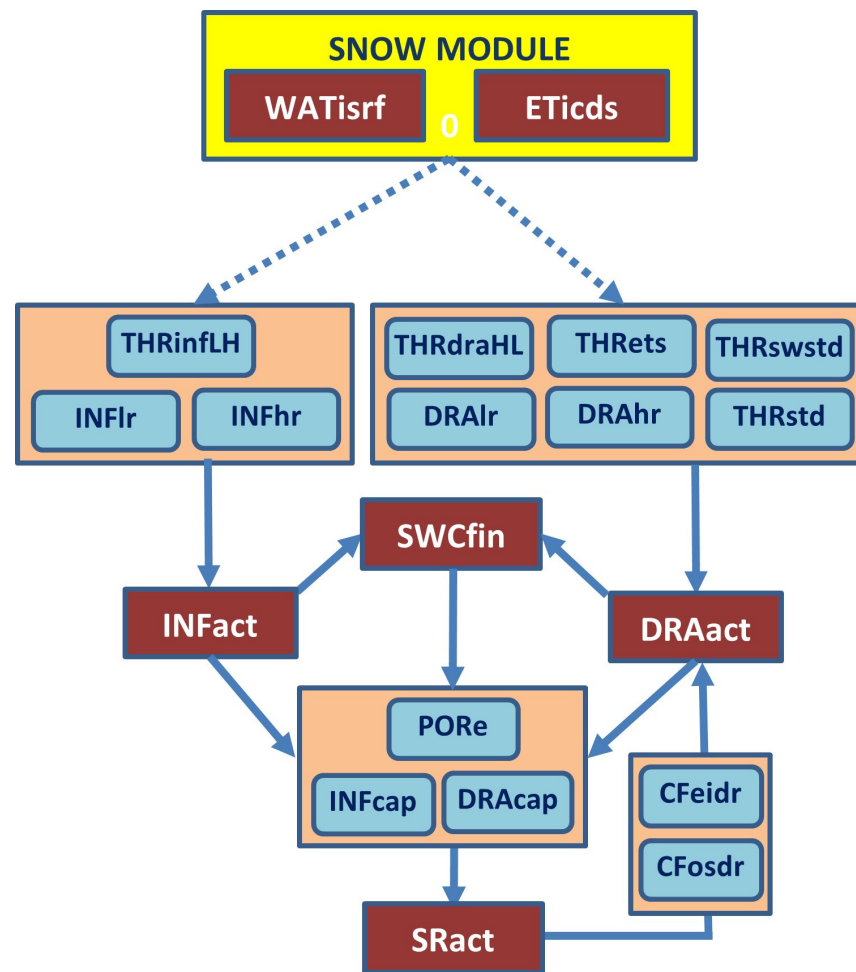

Figure 3. Simplified workflow diagram for the SNOSWAB WATER BALANCE module (yellow box—connection with a different calculation module, orange boxes—module coefficients, red boxes—output variables; WATisrf—water available for infiltration or surface runoff, ETicds—soil ET, THRinfLH—SWC threshold for switching between low and high infiltration rates, INFlr—infiltration rate at low SWC, INFhr—infiltration rate at high SWC, THRdraLH—SWC threshold for switching drainage from high to low rates, THRets—SWC threshold for stopping soil evapotranspiration, THRswstd—SWC threshold for stopping drainage, DRAlr—drainage rate at low SWC, DRAhr—drainage rate at high SWC, THRstd—air temperature threshold for stopping drainage; INFact—actual infiltration, SWCfin—soil water content, DRAact—total drainage, PORe—soil effective porosity, INFcap—infiltration capacity, DRAcap—drainage capacity, SRact—total surface runoff, CFeidr—drainage correction factor for excess infiltration, CFosdr—drainage correction factor for soil oversaturation; dashed lines indicate amounts transferred from the SNOW module).

The SNOSWAB water budget for each time step was calculated in millimeters of water using Equations (1)—(7).

$$IN = OUT + \Delta S + \Delta E \tag{1}$$

$$IN = TOTPP \tag{2}$$

$$TOTPP = RAIN + SNOF = RSI + RSSL \tag{3}$$

$$WATisrf = RSSL + SNMF - ETas \tag{4}$$

$$OUT = SRact + DRact + ETicds \tag{5}$$

$$\Delta S = \Delta SNO + \Delta SWC \tag{6}$$

where

DRact—total drainage;
ETas—evapotranspiration above soil;
ETicds—evapotranspiration in soil;
IN—total inflow into the model;
OUT—total outflow from the model;
RAIN—rainfall amount;
RSI—rain and snowfall contributing to snow layer;
RSSL—rain and snowfall contributing to infiltration;
SNMF—(net) snowmelt;
SNOF—snowfall amount;
SRact—total surface runoff;
TOTPP—total precipitation;
WATisrf—water available for infiltration or surface runoff;
ΔE—model error;
ΔS—change in soil and/or snowpack water storage [$\Delta S = \Delta St_f - \Delta St_i$, where t_f is the last record in the timeseries and t_i is the first record in the timeseries];
ΔSNO—change in snowpack storage;
ΔSWC—change in soil water content.

Using the equations above, the SNOSWAB water budget can be re-written in expanded form as

$$RSSL + SNMF = SRact + DRact + Etas + ETicds + \Delta SNO + \Delta SWC + \Delta E \tag{7}$$

For each simulation, the budget absolute (Equation (8)) and relative (Equation (9)) errors were calculated outside of the SNOSWAB model for both the model output and input data. Based on recommendations from the literature for water balance modeling [54–56], it was considered that the model results are acceptable if the relative error was less than 10%.

$$\Delta E = IN_{ave} - OUT_{ave} - \Delta S \text{ [mm]} \tag{8}$$

$$\Delta E\% = 100 - \frac{INave}{OUTave + \Delta Sfi} \times 100 \text{ [\%]} \tag{9}$$

where

ΔE—absolute model error for the period covered by the timeseries;
$\Delta E\%$—relative model error for the period covered by the timeseries;
IN_{ave}—multi-annual average of inflow into the model;
OUT_{ave}—multi-annual average of outflow from the model.

2.4. SNOSWAB Input Data

The data used in this study were obtained from a 12-year (2008–2019) field study conducted in Field 355 located at the Agriculture and Agri-Food Canada Harrington Experimental Farm (HEF) (46°20′34″ N, 63°09′50″ W) on Prince Edward Island (PEI) in Atlantic Canada as part of a larger research effort aimed at understanding the impact of

intensive agricultural practices associated with potato cropping systems on the quantity and quality of surface and groundwater [48,50,57,58]. The study site is located in a temperate humid climate. The average annual air temperature is 5.7 °C, while the monthly average air temperature reaches its minimum in January (i.e., −7.7 °C) and its maximum in July (i.e., 18.7 °C) [59]. Precipitation is relatively uniformly distributed through the year and equals 1150 mm annually. Snowfall in the area is significant, with 25% of the total precipitation occurring as snow and the snowpack reaching a maximum depth in February, resulting in significant snowmelt between February and April [59]. Previous studies focused on the intra-annual dynamics of snow processes in PEI are limited; however; for example, Bhatti et al. (2021) [60] highlight that the maximum streamflow in several PEI watersheds was estimated to occur between March and May and link this to the snow-dominated hydrological regimes in these watersheds. Edwards et al. (1998) [61] further recognizes the significance of snowmelt processes, indicating that this is responsible for more than half of the total soil erosion from arable land in PEI, while Liao et al. (2005) [62] found that spring snowmelt provides about half of the annual groundwater recharge. The soils at the study site belong to the Charlottetown soil association, the dominant soil association in PEI, have a sandy loam texture and are classified as Orthic Humo-Ferric Podzol [63,64]. The field has been under a three-year potato–barley–clover (PBC) rotation since 2008, with PBC rotation being the most common rotation on PEI [48,57,65].

SNOSWAB operates using a daily timestep, and the input data consist of required data and optional data. The required daily data include mean air temperature (°C); total precipitation (mm); rainfall (mm); and actual evapotranspiration (mm). Optional data include daily timeseries that can be used for calibrating the various routines of the model (UCD—User Calibration Data). UCD are not restricted to specific variables of the model as each available optional timeseries can be paired with a model variable during the calibration process.

Daily mean air temperature, total precipitation and rainfall between 2008 and 2019 were obtained from the Environment and Climate Change Canada Charlottetown weather monitoring station, PEI, Canada [66], which is located about 10 km south of HEF.

Daily evapotranspiration was calculated using the Penman–Monteith, Thornthwaite, Blaney–Criddle, Turc, Priestley–Taylor, Hargreaves, Jensen–Haise and Abtew methods available in ETCalc, another tool included in the HTS [49]. The daily precipitation, air temperature, air relative humidity and wind speed data required for the respective methods were obtained from the Environment and Climate Change Canada Charlottetown weather monitoring station (46°17′24″ N, 63°7′48″ W), PEI, Canada [59], and the daily solar radiation for the location corresponding to the Charlottetown weather station was obtained from NASA's Power Project database [67]. The potential or reference evapotranspiration resulting from the application of each method included in ETCalc was converted to actual evapotranspiration by multiplying the output from each method with the monthly crop coefficients (K). The values of the crop coefficients were set so the multi-annual average of ETA obtained with each method was within ±2% of the multi-annual average obtained using the weekly ETA from the ORNL DAAC MODIS global database [68]. To minimize the bias of individual methods, the average of the daily actual evapotranspiration obtained with each method included in ETCalc was used. More details on the application of ET-Calc used in this study for obtaining the daily actual evapotranspiration are presented in Danielescu, 2023 [49], a study conducted in the same field, during the same period, and dedicated to the estimation of the various evapotranspiration forms.

The UCD datasets (i.e., optional data) used for calibration of SNOSWAB included daily snowpack thickness (cm), soil water content (%), surface runoff (mm) and baseflow (mm). Snowpack thickness (UCD1) was obtained from the Environment and Climate Change Canada Charlottetown weather monitoring station, PEI, Canada [59]. Snowpack thickness was used for calibrating the SNTFcm (i.e., snow layer thickness) SNOSWAB output variable. Soil water content (UCD2) was measured hourly at up to 6 locations distributed across Field 355, using 5TE Decagon sensors connected to EM50 data loggers (METER Group,

Pullman, WA, USA). Soil water content was measured through the soil profile, at four or five depths at each location. The data obtained from the various locations and depths were averaged to obtain a daily timeseries representative of the entire soil profile. The methods for the collection and processing of soil water content data used in this study are presented in detail in Danielescu et al., 2022 [50]. Soil water content was used for calibrating the SWCfin (i.e., soil water content) SNOSWAB output variable. Surface runoff (UCD3) and baseflow (UCD4) were obtained via hydrograph separation, using the methods available in the SepHydro [47] online tool included in the HTS. For this study, the daily streamflow data for a small stream adjacent to Field 355 (i.e., Bell Creek) were used. For minimizing the bias of each method, the average of the daily output with each of the 11 algorithms available in SepHydro was used for obtaining the daily surface runoff and baseflow for the calibration of SNOSWAB. Surface runoff was used for calibrating the SRact (i.e., total surface runoff) SNOSWAB output variable, and baseflow was used for calibrating the DRAact (i.e., total soil drainage) SNOSWAB output variable. While there are conceptual differences between surface runoff and drainage at the field scale and surface runoff and baseflow generation at the watershed scale, this was considered a reasonable approach in the absence of alternative calibration data, at least for larger temporal scales (e.g., monthly or annual basis). More details regarding the hydrograph separation methods included in SepHydro and the SepHydro calibration are available in Danielescu et al., 2018 [47] and Danielescu et al., 2024 [48].

2.5. SNOSWAB Model Calibration and Validation

SNOSWAB was calibrated using data collected from Field 355 between 2010 and 2014 (i.e., 5 years). Following the calibration, the model was validated by using data collected from the same location between 2015 and 2019 (i.e., 5 years). The objective of SNOSWAB calibration was to achieve moderate or high fitness for various time intervals between the SNOSWAB model output and the four UCD timeseries available (i.e., snow layer thickness, soil water content, surface runoff and drainage). The objective of the validation was to evaluate the performance of the calibrated model using a data set that was different from the one used for the calibration. The model was run using the daily timestep, and the model output was analyzed using daily, monthly calendar season and yearly time intervals. In addition, multi-year averages for each day and month of the year were calculated.

The calibration consisted of adjusting the various model coefficients (six coefficients for the SNOW module and 14 coefficients for the WATER BALANCE module) and was conducted by trial and error until no further improvement in model fitness was obtained. The initial values (i.e., values for the first day of the simulation) required by the model for certain parameters or variables (i.e., snow layer thickness, snowmelt, SWC, net SWC gain and loss, surface runoff) were obtained from the UCD data, or assumed to be zero if the respective data were not available. The validation simulation was performed using the values of the various coefficients obtained from the calibration and the timeseries for the validation period. The model fitness was assessed using univariate (e.g., average) and bivariate statistics (i.e., R^2—coefficient of determination, NRMSE—Normalized Root-Mean-Square Error, PBIAS—Percentage Bias) (Equations (10)–(13)) for various time intervals. R^2 was considered to be indicative of low model performance when $R^2 < 0.3$, moderate performance when $0.3 < R^2 < 0.5$ and high performance when $R^2 > 0.5$, in accordance with the threshold values suggested by Cohen (1988) [69]. NRMSE was considered to be indicative of low model performance when NRMSE > 70%, moderate performance when 50% < NMRSE < 70% and high performance when NRMSE < 50%. PBIAS was considered to be indicative of low model performance when PBIAS < −50% or PBIAS > 50%, moderate performance when −50% < PBIAS < −25% or 25% < PBIAS < 50% and high performance when −25% < PBIAS < 25%. The NRMSE and PBIAS threshold values were based on Moriasi et al. (2007) [70]. Of note, studies including ranges of values for the above statistics at the field scale for the four UCD timeseries at various timesteps are limited, and hence,

preference was given to using ranges of values generally applicable to the modeling of hydrological processes.

$$R^2 = \left(\frac{\sum (Y_{iME} - Y_{ME\_AVE})(Y_{iMO} - Y_{MO\_AVE})}{\sqrt{\sum (Y_{iME} - Y_{ME\_AVE})^2 \sum (Y_{iMO} - Y_{MO\_AVE})^2}} \right)^2 \tag{10}$$

In the Equation (10),
R^2—the coefficient of determination;
Y_{iME}—the ith measured value (i.e., observed);
Y_{ME_AVE}—the average of the measured values (i.e., observed);
Y_{iMO}—the ith value predicted by the model (i.e., modeled);
Y_{MO_AVE}—the average of the values predicted by the model (i.e., modeled).

$$RMSE = \sqrt{\frac{\sum_{i=1}^{n}(Y_{iME} - Y_{iMO})}{n}} \tag{11}$$

In the Equation (11),
RMSE—the Root Mean Square Error;
Y_{iME}—the ith measured value (i.e., observed);
Y_{iMO}—the ith value predicted by the model (i.e., modeled);
n—the number of available data points.

$$NRMSE = \frac{RMSE}{Y_{ME\_MAX} - Y_{ME\_MIN}} \tag{12}$$

In the Equation (12),
NRMSE—the Normalized Root Mean Square Error;
Y_{ME_MAX}—the maximum measured value (i.e., observed);
Y_{ME_MIN}—the minimum measured value (i.e., observed).

$$PBIAS = \frac{\sum_{i=1}^{n}(Y_{iME} - Y_{iMO})}{\sum_{i=1}^{n} Y_{iME}} \times 100 \tag{13}$$

In the Equation (13),
PBIAS—Percentage Bias (%);
Y_{iME}—the ith measured value (i.e., observed);
Y_{iMO}—the ith value predicted by the model (i.e., modeled).

3. Results and Discussion

3.1. Model Calibration

The final values of the various parameters adjusted during SNOSWAB model calibration are shown in Table 1, with more details about each parameter provided in Table S1 in the Supplementary Materials.

When considering the output of the model for various time steps and averaging intervals, the bivariate statistics indicated high model performance in most cases (Table 2, Table S4 in Supplementary Materials), as also evidenced by the examples shown in Figure 4.

Both PBIAS and NRMSE were in the high-model-performance range for all User Calibration Datasets (UCDs) and all intervals, suggesting minimal bias as well as minimal error for the calibrated model simulation (Table 2, Table S4 in Supplementary Materials). When considering the average PBIAS for all intervals for each UCD, the best model fitness was obtained for surface runoff (SRact, 2.09%), followed by soil water content (SWCfin, −3.98%), drainage (DRAact, 7.01%) and snow layer thickness (SNTFcm, 14.1%). Correspondingly, NRMSE showed that the best model performance was achieved for SNTFcm (11.2%), followed by SWCfin (19.3%), SRact (21.4%) and DRAact (23.1%).

Table 1. Values of model parameters for the calibrated model.

SNOW Module	*Value*
Initial Values	
SNWTinit—Initial snow layer thickness (cm)	4.0
SNWMinit—Initial snowmelt (mm)	0.0
Coefficients	
THRrs—Air temperature threshold for rain to be accumulated as snow ((°C)	−2.5
THRsm—Air temperature threshold for initiating snowmelt ((°C)	0.5
CFTsm—Correction factor: snowmelt due to air temperature (mm)	3.2
CFRsm—Correction factor: snowmelt due to rain (mm)	1.5
CFSmc—Correction factor: convert mm of snow to cm of snow	0.72
CFets—Correction factor: portion of evapotranspiration occurring in the soil	0.70
SOIL WATER Module	
Initial Values	
SWCinit—Soil water content (SWC) (% of PORe)	90
SRinit—Surface runoff (mm)	0
NGinit—Net SWC gain (mm)	0
NLinit—Net SWC loss (mm)	0
Layer Properties	
THKN—Layer or root zone thickness (mm)	1000
PORe—Layer effective porosity (%)	33.0
Infiltration Coefficients	
THRinfLH—SWC threshold for switching between low and high infiltration rates (% POre)	90
INFlr—Infiltration rate at low SWC (mm hr^{-1})	1.5
INFhr—Infiltration rate at high SWC (mm hr^{-1})	0.2
Drainage Coefficients	
THRdraHL—SWC threshold for switching drainage from high to low rates (% PORe)	85
DRAlr—Drainage rate at low SWC (mm hr^{-1})	0.005
DRAhr—Drainage rate at high SWC (mm hr^{-1})	0.07
THRswstd—SWC threshold for stopping drainage (% PORe)	55
THRtstd—Air temperature threshold for stopping drainage (°C)	−6.67
CFeidr—Drainage boost correction factor 1: portion of water from excess infiltration rerouted to drainage	0.50
CFosdr—Drainage boost correction factor 2: portion of water from oversaturation rerouted to drainage	0.15
Other Coefficients	
THRets—SWC threshold for stopping soil evapotranspiration (% PORe)	60
THRlw—Threshold for low SWC state (% PORe)	70
THRhw—Threshold for high SWC state (% PORe)	90

Table 2. Model performance statistics for SNOSWAB calibration and validation [1] simulations.

	Snow Thickness (cm) [SNTFcm]	Soil Water Content (%) [SWCfin]	Surface Runoff (mm) [SRact]	Drainage (mm) [DRAact]
Daily				
Average UCD data	8.48 [10.3]	26.6 [27.5]	0.58 [0.56]	1.55 [1.53]
Average model output	7.22 [10.9]	27.7 [27.7]	0.57 [0.48]	1.45 [1.34]
PBIAS (%)	14.9 [−6.12]	−4.04 [−0.54]	1.88 [14.0]	6.91 [12.5]
NRMSE (%)	7.73 [2.84]	12.1 [10.9]	11.2 [15.4]	22.3 [21.2]
R^2	0.83 [0.98]	0.64 [0.75]	0.10 [0.17]	0.07 [0.13]
Monthly				
Average UCD data	8.65 [10.4]	26.6 [27.6]	17.6 [16.9]	47.3 [46.7]
Average model output	7.38 [11.0]	27.7 [27.7]	17.2 [14.5]	44.0 [40.9]
PBIAS (%)	14.7 [−6.16]	−4.01 [−0.51]	1.88 [14.0]	6.91 [12.5]
NRMSE (%)	7.54 [2.47]	14.3 [10.8]	16.0 [19.4]	14.6 [14.5]
R^2	0.89 [0.99]	0.74 [0.87]	0.33 [0.56]	0.42 [0.53]
Yearly				
Average UCD data	8.65 [10.4]	26.6 [27.6]	211 [203]	568 [560]
Average model output	7.38 [11.0]	27.7 [27.7]	207 [174]	528 [491]
PBIAS (%)	14.7 [−6.16]	−4.01 [−0.51]	1.88 [14.0]	6.91 [12.5]
NRMSE (%)	31.4 [5.85]	46.8 [20.4]	29.8 [51.8]	27.6 [39.6]
R^2	0.54 [1.00]	0.38 [0.80]	0.70 [0.72]	0.58 [0.85]

Note: [1] validation simulation values are shown in brackets.
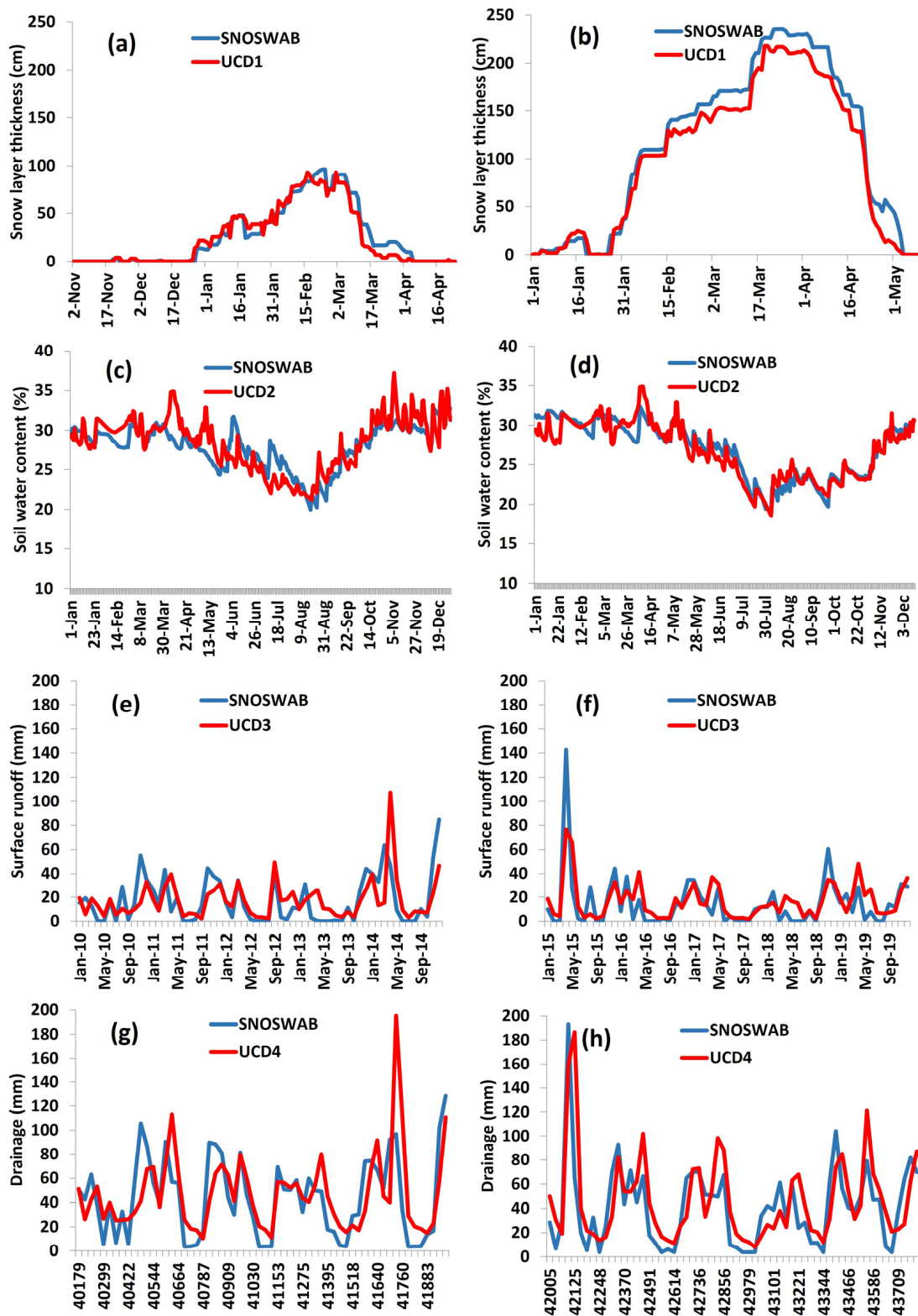
Figure 4. Examples of comparisons between UCD and SNOSWAB model outputs for the calibration (left) and validation (right) simulations. (**a**) Daily snow layer thickness (winter 2010/11); (**b**) daily snow layer thickness (winter 2014/15); (**c**) daily soil water content (2010); (**d**) daily soil water content (2017); (**e**) monthly surface runoff (2010–2014); (**f**) monthly surface runoff (2015–2019); (**g**) monthly drainage (2010–2014); (**h**) monthly drainage (2015–2019).

The coefficient of determination showed a wider range of values for both the various UCDs and intervals. Thus, R^2 had values between 0.54 and 0.99 for snow layer thickness (SNTFcm), suggesting high performance of the model for all averaging intervals. For soil water content (SWCfin), R^2 suggested high model performance for all averaging intervals (i.e., $0.74 < R^2 < 0.95$) except for yearly time interval averaging (i.e., $R^2 = 0.38$; moderate performance). The difference in SWC between the model output and UCD was less than 0.1%, regardless of the averaging interval considered. SRact and drainage DRAact had the lowest overall R^2 values when compared to the other UCDs (Table 2, Table S4 in Supplementary Materials). SRact suggested high performance of the model for yearly ($R^2 = 0.70$), moderate performance for monthly ($R^2 = 0.33$), calendar season ($R^2 = 0.49$) and multi-year monthly averages ($R^2 = 0.33$), and low performance for daily ($R^2 = 0.10$) and multi-year daily averages ($R^2 = 0.08$). With slightly better R^2 values than SRact, DRAact suggested high performance of the model for calendar season ($R^2 = 0.59$) and yearly ($R^2 = 0.58$) averages, moderate performance for monthly ($R^2 = 0.42$) and multi-year monthly ($R^2 = 0.45$) averages, and low performance for all other averaging intervals. The generally lower SRact and DRAact R^2 values for the smaller time intervals can be attributed in part to the methodology used for obtaining the corresponding UCDs. The UCDs used for calibrating surface runoff and drainage were obtained from hydrograph separation (i.e., surface runoff and baseflow contributions to streamflow). Both UCDs are continuous (i.e., no zero values) and representative of watershed scale processes and, hence, both have slower and smoother response times compared to SRact and DRAact, which are discontinuous (i.e., can have zero values) and controlled by field-scale processes.

3.2. Model Validation

With respect to the SNOSWAB input timeseries, the validation period was colder, with more snowfall and less rainfall, compared to the calibration period. The validation period was about 10% colder than the calibration period (Table 3), with the minimum monthly temperature ~60% lower than the corresponding value for the calibration period (i.e., February 2015 vs. January 2013). Although the amount of precipitation for the validation period was only 6.2% lower than the equivalent amount for the calibration period, the amount of rainfall was 44% lower than for the calibration period. Conversely, the amount of snowfall for the validation period was 11.8% higher than for the calibration period, with the maximum monthly snowfall amount being 42.2% larger for the validation period (i.e., February 2015 vs. February 2011). The month with the maximum precipitation for the validation period (i.e., November 2018) was 41% lower than the maximum measured for the calibration period (i.e., October 2011). Therefore, it was considered that the validation period was meteorologically distinct from the calibration period and, hence, it was suitable for assessing SNOSWAB performance.

Table 3. Annual values for SNOSWAB input timeseries for the calibration and validation [1] simulations.

Year	Air Temperature (°C)	Precipitation (mm)	Rain (mm)	Snow (mm)	ET Total (mm)
2010 [2015]	7.5 [5.3]	1354 [1402]	1165 [893]	189 [509]	588 [556]
2011 [2016]	6.6 [6.5]	1370 [1096]	1081 [824]	289 [272]	561 [561]
2012 [2017]	7.3 [6.4]	1079 [1093]	847 [866]	232 [227]	608 [578]
2013 [2018]	5.9 [5.9]	1159 [1203]	913 [977]	247 [227]	562 [570]
2014 [2019]	5.9 [5.6]	1454 [1227]	1154 [1057]	300 [170]	563 [554]
Average	6.6 [5.9]	1283 [1204]	1032 [923]	251 [281]	576 [564]
Minimum	−8.0 [−12.6]	28.0 [24.1]	7.1 [2.6]	0.0 [0.0]	3.1 [3.7]
Maximum	21.3 [21.3]	321 [189]	315 [174]	119 [169]	136 [135]

Note: [1] validation simulation values are shown in brackets.

Similar to the calibration simulation, the bivariate statistics for the validation simulation indicated high model performance in most cases (Table 2, Table S4 in Supplementary Materials), and this finding is further illustrated by the examples shown in Figure 4.

PBIAS was in the high-model-performance range for all UCDs and all averaging intervals, suggesting minimal bias for the validation simulation. NRMSE was in the high-model-performance range for all UCDs and all averaging intervals, except for SRact for the yearly averaging interval, when the model showed moderate performance. When considering the average PBIAS for all intervals and for all UCDs, the best model fitness was obtained for SWCfin (-0.52%), followed by SNTFcm (-6.04%), DRAact (12.4%) and SRact (14.0%). Correspondingly, NRMSE showed that the best model performance was achieved for SNTFcm (3.88%), followed by SWCfin (11.7%), DRAact (22.6%) and SRact (24.9%). Similar to the calibration simulation, the coefficient of determination showed a wider range of values for the various UCDs and averaging intervals. Thus, R^2 had values between 0.98 and 1.00 (i.e., high performance) for SNTFcm, suggesting better performance of the model than for the calibration simulation. For SWCfin, R^2 ranged between 0.75 and 0.95, with all values suggesting high model performance, as well as indicating better performance of the model than for the calibration simulation. Similar to the calibration simulation, SRact and DRAact had the lowest overall R^2 values when compared to the other UCDs. When considering the average for all time intervals for each of these UCDs, the average R^2 was higher than for the calibration simulation (i.e., 0.50 vs. 0.34 for SRact and 0.51 vs. 0.37 for DRAact), suggesting a better fit for the validation simulation than for the calibration simulation.

The average PBIAS for all UCDs and for all averaging intervals was 4.97%, which was 1.84% lower (i.e., better) than the corresponding PBIAS obtained for the calibration simulation (i.e., 6.81%), thus suggesting a 37.0% relative improvement in model performance when compared to the calibration simulation. The nMRSE corresponding average showed a decrease of 3.03% (i.e., 15.8% for the validation simulation vs. 18.8% for the calibration simulation), thus suggesting a relative improvement of 19.2% for the validation simulation. R^2 showed a 19.7% relative improvement for the validation simulation (i.e., 0.71 vs. 0.57). The SNOSWAB water budget error for the validation simulation was 26.3 mm (i.e., 2.2%), which was in the same range as the budget error for the calibration simulation (i.e., 42.3 mm or 3.3%). For both the calibration and simulation cases, the SNOSWAB budget error was smaller than the budget error calculated using the UCD data (i.e., UCD data budget errors of 6% for the calibration simulation and 10.5% for the validation simulation, respectively). Overall, the output from the validated model showed similar fitness with UCDs when compared to the output from the calibration simulation.

Thus, the high performance of the calibrated model, as evidenced by the results of the multi-pronged calibration and validation procedures, attests to the capability of the SNOSWAB model to accurately simulate key hydrological process, including snow layer dynamics, soil water content and, consequently, soil water budget terms. Although only the four variables for which calibration data existed were discussed here, it is reasonable to assume that the other processes simulated by SNOSWAB (i.e., the accumulation of rain and snow into the snowpack; snow melting controlled by air temperature and rainfall events; infiltration; the impact of soil dryness/wetness on evapotranspiration, surface runoff generation and drainage; surface runoff resulting from soil oversaturation; and the evaluation of crop water deficit or excess) provide reasonable estimates; however, further calibration and validation should be conducted for cases where the respective datasets are available.

3.3. Model Output

In order to obtain estimates representative of the entire study period (2008–2019), a new simulation was set up using the values of the parameters obtained during calibration and the complete 12-year input dataset. The dynamics of the key output variables for the SNOW and WATER BALANCE modules are shown in Figures 5 and 6 and Tables S5–S8 in the Supplementary Materials.
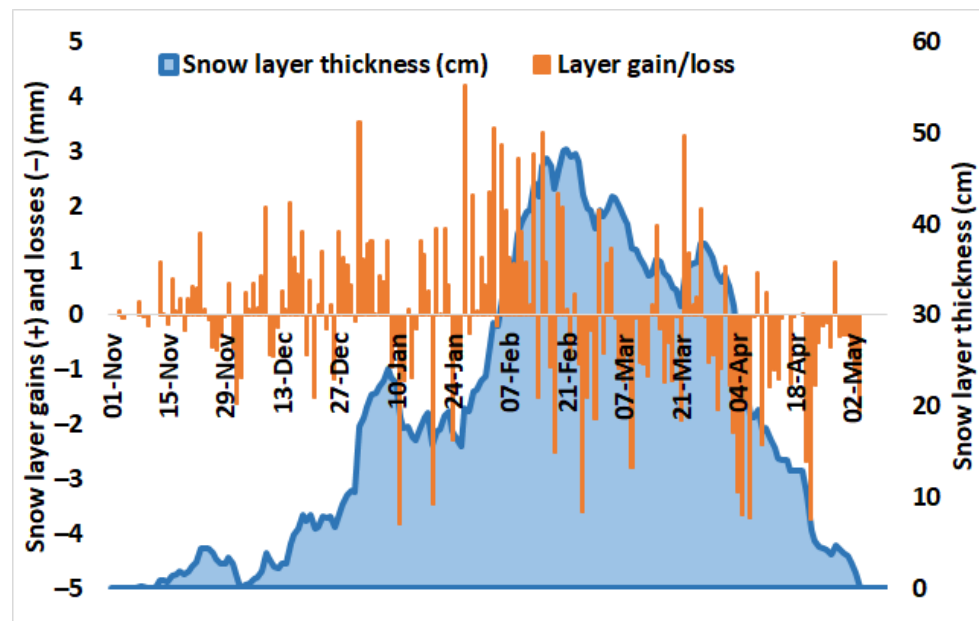
Figure 5. Multi-year daily averages for snow layer thickness and net snow layer gains and losses.
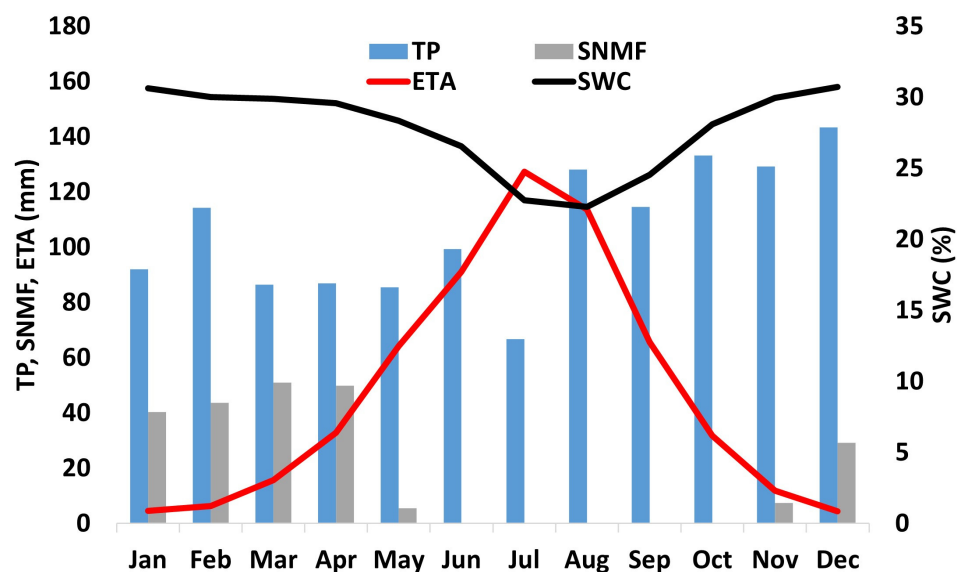

Figure 6. Multi-year monthly averages for total precipitation (TP), snowmelt (SNMF), actual evapotranspiration (ETA) and soil water content (SWC).

3.3.1. Snow Processes

As expected, the snow gains dominated the first part of the winter (November to mid-February), while the snowmelt processes were prevalent during the later part of the cold season (Figure 5). Overall, ~225 mm of water entered and left the snowpack annually on average for the study period. When considering the entire period of study, the snow could have been present on the ground between 1 November and 3 May, although significant variation was observed from year to year. Based on multi-year monthly averages, snow layer thickness reached its monthly maximum in February (40.2 cm average) followed by March (36.9 cm). Snow layer gain (i.e., 167.9 mm for February 2015), snowmelt (i.e., 271 mm for April 2015) and snow layer thickness (i.e., 278.5 cm for March 2015) reached their monthly maximum for the study period during the winter of 2014–2015 (Table S5 in Supplementary Materials). The winters of 2009–2010, 2012–2013, 2017–2018 and 2018–2019 were the years when snow-related processes had reduced magnitude. For example, for the winter of 2012–2013, the cumulative snow layer gain between

December and February was 80.8 mm, the snowmelt was 70.6 and the average snow layer thickness was 10.0 cm. The magnitude of the snow-related processes confirms the significance of these processes with respect to their role in controlling SWC, groundwater recharge, baseflow and surface runoff formation [56,62] and implicitly suggests their significance in the surface and subsurface transport of various contaminants.

3.3.2. Soil Water Content

The average SWC for the entire period was 27.8%. Similar to the measured data, SWC was high during the winter and early spring, due to minimal evapotranspiration combined with low temperatures and the presence of the snowpack (Figure 6). Starting with mid-spring, the SWC values started to decrease and reached their lowest during the summer (Figure 6), driven by the increased evapotranspiration and reduced amounts of precipitation. In the fall, downward-trending evapotranspiration in conjunction with upward-trending precipitation contributed to increased SWC for the cold season. Although SWC showed the same intra-annual trends for each of the years of the study period, as was the case with snowpack processes, its dynamics showed variability from year to year. Thus, the lowest SWC values were estimated for 2017 (26.9%), 2012 (27.1%) and 2016 (27.2%). Conversely, the highest SWC values were estimated for 2009 (28.6%), 2008 (28.4%) and 2019 (28.3%). SWC is a result of the complex interactions among various factors, including precipitation amount, snow layer thickness and snowmelt, air temperature, and evapotranspiration. On an annual basis, SWC showed a moderate correlation only with the total amount of precipitation ($R^2 = 0.49$) and a low correlation with the other parameters. However, on a monthly basis, SWC showed a high correlation with both evapotranspiration ($R^2 = 0.73$) and air temperature ($R^2 = 0.69$).

The analysis of soil water stress (i.e., water deficit or water excess), conducted in the context the study site used for potato cropping, revealed that based on the multi-year monthly averages, the months with most days with low SWC (i.e., SWC < 0.7 PORe) were July (17.8 days) and August (21.0 days) (Figure 7). On an annual basis, for the study period, SWC was on average in the optimal range for 163 days, in the low range for 53.2 days and in the high range for 149 days. During the potato growing season (25 May to 30 October; 159 days), SWC was in the low range for 53.2 days, the optimal range for 92.4 days and the high range for 13.4 days, suggesting that crops experienced water deficit for a significant portion of the growing season. This finding is similar to previous estimates reported in the literature [49,50,71,72], which suggested that supplemental irrigation in the area could be beneficial for potato crops, particularly during the drier years.
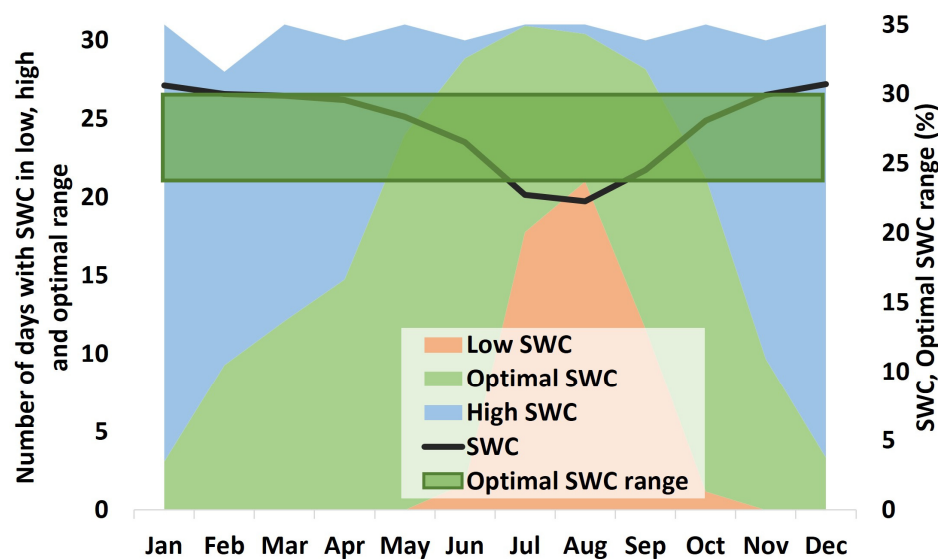

Figure 7. Multi-year monthly averages for number of days with soil water content (SWC) in low, high and optimal ranges for potato crop.

3.3.3. Soil Water Budget

For the entire study period (2008–2019), precipitation averaged 1280 mm y^{-1}, and the largest soil water losses were through drainage (527 mm y^{-1} or 41.2 % of precipitation) and evapotranspiration from the soil (440.7 mm y^{-1} or 34.4 % of precipitation), followed by surface runoff (205 mm y^{-1} or 16.0 % of precipitation) and evapotranspiration above the soil (129 mm y^{-1} or 10.0 % of precipitation). The changes in water storage either in the soil or in the snowpack were relatively small (i.e., −17.8 mm and −61.1 mm between the first and last days of the study period, respectively). Studies on soil water budget in PEI are scarce, and hence, comparison was possible in most cases only by using proxy information. Considering these limitations, the SNOSWAB estimates of the various soil water budget terms were in a similar range to the values reported in the literature. For example, Francis, 1989 [73], estimated that baseflow to streams, which, with some limitations (see Section 2.3), can be used for comparison with soil drainage, ranged between 22 and 42%, and evapotranspiration ranged between 30 and 40% of annual precipitation for various watersheds in PEI. Paradis et al., 2016 [74] estimated higher values for evapotranspiration (i.e., 50% of precipitation; 583 mm) and found that surface runoff represents about 19% of total precipitation (i.e., 221 mm), while drainage represents about 31% of precipitation (i.e., 369 mm), in a study conducted at the PEI scale.

Infiltration into the soil, estimated after surface runoff (i.e., 205 mm y^{-1}) and evapotranspiration above the soil (i.e., 128.5 mm y^{-1}) were removed from the available water, but before evapotranspiration (i.e., 441 mm y^{-1}) from the soil was considered, averaged 967 mm y^{-1} for the study period. While PEI soils are recognized for having high infiltration and low surface runoff potential [57,75], studies aimed at quantifying infiltration in this area are limited. When multi-year monthly averages were considered, infiltration during the summer generally had high values, except for July, when it was impacted by the reduced amount of precipitation (Figure 8). Despite the relatively high summer values for infiltration, drainage reached its minimum during this period (i.e., 18.1 mm in June, 5.7 mm in July and 13.2 mm in August) as it is apparent that evapotranspiration from the soil (i.e., 79.6 mm in June, 94.8 mm in July and 71.0 mm in August) was the main driver for the amount of water available in the soil for storage and drainage. Surface runoff also reached its minimum during the summer months (i.e., 3.3 mm in June, 0.4 mm in July and 8.1 mm in August). The key soil water budget terms, together with the dynamics of soil water content, confirmed that the soils experienced water deficit during the growing season, and this can be detrimental to the growth of crops and natural vegetation [50,76,77]. The low values of drainage during the summer are considered the leading cause of reduced groundwater recharge during the summer, which can impact the baseflow of streams [57,73,78].
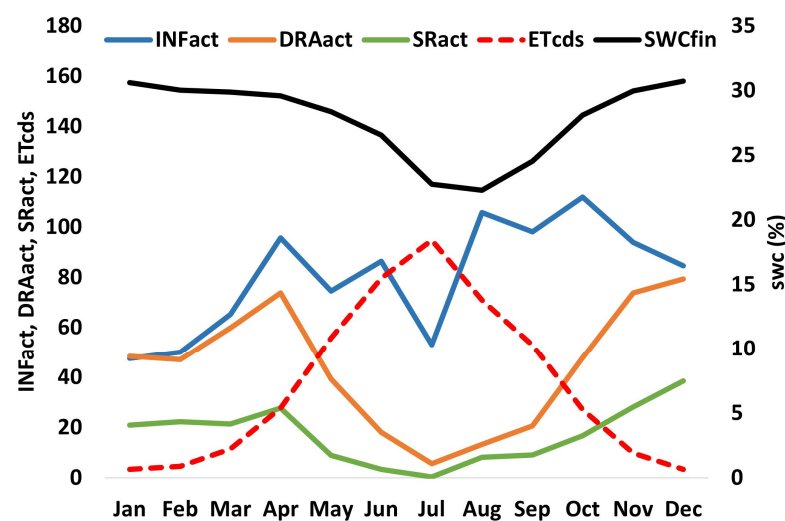

Figure 8. Multi-year monthly averages of key soil water budget terms (INFact—infiltration; DRAact—drainage; SRact—surface runoff; ETcds—soil evapotranspiration; SWC fin—soil water content).

4. Conclusions

Here, the SNOSWAB (<u>Sno</u>w, <u>S</u>oil <u>W</u>ater and <u>W</u>ater <u>B</u>alance) model was presented. SNOSWAB is a unique, free, online tipping-bucket (or capacity) deterministic model (https://snoswab.hydrotools.tech; accessed on 15 May 2024) that can be used for understanding the daily dynamics of selected snowpack processes, soil water content and soil water budget terms. SNOSWAB is most suitable for modeling field-scale processes for vertically and horizontally homogeneous soils, and its applicability is not limited to specific climate zones or geographical areas. SNOSWAB provides a streamlined interface; flexibility in adjusting the coefficients used by each of its modules; visualization, export and import capabilities; and powerful calibration routines. These elements, together with its unrestricted applicability to specific climate zones or geographical areas, show promise that the model it can be adopted as an alternative for or support the development of more complex, standalone models that might require extensive resources and expertise, either through the generation of critical data for or through integration into such models.

SNOSWAB can potentially appeal to a diverse user base, including academia, industry, environmental groups and the public at large, as it can be used for a broad range of applications, including studies aimed at understanding, for example, the impact of weather on various soil water balance components and on crop water stress, or the impact of agricultural practices such as irrigation on the movement of water and contaminants in the subsurface.

The high performance of the model was confirmed through the calibration and validation procedures conducted using a 12 year daily data set (2008–2019) collected from an agricultural field located at AAFC's Harrington Experimental Farm on Prince Edward Island (PEI), Canada. In addition, the results of the application of the SNOSWAB model provide insight into a series of hydrological processes which are currently under-studied in PEI. While the maritime temperate–humid climate of PEI provided significant variability in the various weather parameters used in the model (e.g., precipitation regimes ranging from extreme rainfall or snowfall events to prolonged dry or wet spells, winter snow cover ranging from bare ground to significant snowpack thickness or periods of canicular weather, and periods of extremely low temperatures), testing of the model's robustness and adaptability will greatly benefit from additional case studies in varying geographical and climatic conditions.

Future SNOSWAB development plans include the implementation of multiple soil layers, integration routines accounting for water additions and losses (e.g., irrigation, ditches, tile drains, etc.), the implementation of autocalibration routines and the refinement of data quality-checking algorithms. Moreover, the development of intercomparisons with existing models would be beneficial for SNOSWAB's further development.

References

1. National Aeronautics and Space Administration [NASA]. Soil Moisture. 1999. Available online: https://weather.ndc.nasa.gov/landprocess/ (accessed on 5 February 2024).
2. Gardner, C.M.K.; Robinson, D.; Blyth, K.; Cooper, J.D. Chapter 1. Soil water content. In *Soil and Environmental Analysis*; Physical Methods, Revised, and Expanded; Smith, K.A., Mullins, C.E., Eds.; CRC Press: Boca Raton, FL, USA, 2000; 660p. [CrossRef]
3. Parkin, G.W. Water budget in soil. In *Encyclopedia of Soil Science*; Chesworth, W., Ed.; Springer: Dordrecht, The Netherlands, 2008; pp. 811–813. [CrossRef]
4. Kirkham, M.B. *Principles of Soil and Plant Water Relations*; Elsevier Academic Press Inc.: Oxford, UK, 2014; 479p. [CrossRef]
5. Iwata, Y.; Hayashi, M.; Hirota, T. Comparison of Snowmelt Infiltration under Different Soil-Freezing Conditions Influenced by Snow Cover. *Vadose Zone J.* **2008**, *7*, 79–86. [CrossRef]
6. Nouri, M.; Homaee, M. Spatiotemporal changes of snow metrics in mountainous data-scarce areas using reanal-yses. *J. Hydrol.* **2021**, *603*, 126858. [CrossRef]
7. Qin, Y.; Abatzoglou, J.T.; Siebert, S.; Huning, L.S.; AghaKouchak, A.; Mankin, J.S.; Hong, C.; Tong, D.; Davis, S.J.; Mueller, N.D. Agricultural risks from changing snowmelt. *Nat. Clim. Change* **2020**, *10*, 459–465. [CrossRef]
8. Qin, Y.; Hong, C.; Zhao, H.; Siebert, S.; Abatzoglou, J.T.; Huning, L.S.; Sloat, L.L.; Park, S.; Li, S.; Munroe, D.K.; et al. Snowmelt risk telecouplings for irrigated agriculture. *Nat. Clim. Change* **2022**, *12*, 1007–1015. [CrossRef]
9. Bittelli, M. Measuring Soil Water Potential for Water Management in Agriculture: A Review. *Sustainability* **2010**, *2*, 1226–1251. [CrossRef]
10. Stark, J.; Thornton, M.; Nolte, P. (Eds.) *Potato Production Systems*; Springer International Publishing: Berlin/Heidelberg, Germany, 2020; p. 635. ISBN 978-3-030-39156-0.
11. Russell, J.L. Scientific research in soil drainage. *J. Agric. Sci.* **1934**, *24*, 544–573. [CrossRef]
12. Dou, X.; Shi, H.; Li, R.; Miao, Q.; Yan, J.; Tian, F. Evaluating the Effects of Controlled Drainage on Nitrogen Uptake, Utilization, Leaching, and Loss in Farmland Soil. *Agronomy* **2023**, *13*, 2936. [CrossRef]
13. Sophocleous, M.A. Combining the soilwater balance and water level fluctuation methods to estimate natural groundwater recharge: Practical aspects. *J. Hydrol.* **1991**, *124*, 229–241. [CrossRef]
14. Wang, H.; Gao, J.; Li, X.; Wang, H.; Zhang, Y. Effects of Soil and Water Conservation Measures on Groundwater Levels and Recharge. *Water* **2014**, *6*, 3783–3806. [CrossRef]
15. Van der Perk, M. *Soil and Water Contamination*; CRC Press: Boca Raton, FL, USA, 2017; 428p. [CrossRef]
16. Pignatello, J.J.; Katz, B.G.; Li, H. Sources, Interactions, and Ecological Impacts of Organic Contaminants in Water, Soil, and Sediment: An Introduction to the Special Series. *J. Environ. Qual.* **2010**, *39*, 1133–1138. [CrossRef] [PubMed]
17. Jin, Y.; Flurry, M. Fate and transport of viruses in porous media. *Adv. Agron.* **2002**, *77*, 39–102. [CrossRef]
18. Meng, L.; Quiring, S.M. A comparison of soil moisture models using soil climate analysis network observations. *J. Hydrometeorol.* **2008**, *9*, 641e659. [CrossRef]
19. Bittelli, M. Measuring Soil Water Content: A Review. *HortTechnology* **2011**, *21*, 293–300. [CrossRef]
20. Haj-Amor, Z.; Araya, T.; Acharjee, T.K.; Bouri, S.; Anlauf, R. Soil-water modeling as a tool for sustainable soil resources management: Progress and future directions. In *Water, Land, and Forest Susceptibility and Sustainability*; Chatterjee, U., Pradhan, B., Kumar, S., Saha, S., Zakwan, M., Eds.; Elsevier Academic Press: Amsterdam, The Netherlands, 2023; pp. 71–96. [CrossRef]
21. Akinremi, O.O.; McGinn, S.M. Usage of soil moisture models in agronomic research. *Can. J. Soil. Sci.* **1995**, *76*, 285–295. [CrossRef]
22. Connolly, R.D. Modelling effects of soil structure on the water balance of soil-crop systems: A review. *Soil. Till. Res.* **1998**, *48*, 1–19. [CrossRef]
23. Ascough, J.C., II; Ahuja, L.R.; McMaster, G.S.; Ma, L.; Andales, A.A. Agriculture Models. In *Encyclopedia of Ecology*; Jørgensen, S.E., Fath, B.D., Eds.; Academic Press: Oxford, UK, 2008; pp. 85–95. [CrossRef]
24. Ranatunga, K.; Nation, E.R.; Barratt, D.G. Review of soil water models and their applications in Australia. *Environ. Modell. Softw.* **2008**, *23*, 1182–1206. [CrossRef]
25. Subbaiah, R. A review of models for predicting soil water dynamics during trickle irrigation. *Irrig. Sci.* **2013**, *31*, 225–258. [CrossRef]

26. Jones, J.W.; Antle, J.M.; Basso, B.O.; Boote, K.J.; Conant, R.T.; Foster, I.; Godfray, H.C.J.; Herrero, M.; Howitt, R.E.; Janssen, S.; et al. Brief history of agricultural system models. *Agric. Syst.* **2016**, *155*, 240–254. [CrossRef] [PubMed]

27. Jones, J.W.; Antle, J.M.; Basso, B.O.; Boote, K.J.; Conant, R.T.; Foster, I.; Godfray, H.C.J.; Herrero, M.; Howitt, R.E.; Janssen, S.; et al. Toward a new generation of agricultural system data, models, and knowledge products: State of agricultural systems science. *Agric. Syst.* **2017**, *155*, 269–288. [CrossRef]

28. Pereira, L.S.; Paredes, P.; Jovanovic, N. Soil water balance models for determining crop water and irrigation requirements and irrigation scheduling focusing on the FAO56 method and the dual Kc approach. *Agric. Water Manag.* **2020**, *241*, 106357. [CrossRef]

29. Šimůnek, J.; Šejna, M.; Brunetti, G.; van Genuchten, M.T. The HYDRUS Software Package for Simulating the One-, Two-, and Three-Dimensional Movement of Water, Heat, and Multiple Solutes in Variably-Saturated Porous Media. Technical Manual I. Hydrus 1D, Version 5.x. 2022. Available online: https://www.pc-progress.com/downloads/Pgm_Hydrus3D5/HYDRUS_Technical_Manual_1D_V5.pdf (accessed on 13 March 2024).

30. Arnold, J.G.; Srinivasan, R.; Muttiah, R.S.; Williams, J.R. Large-area hydrologic modeling and assessment: Part I. model development. *J. Am. Water Res. Assoc.* **1998**, *34*, 73–89. [CrossRef]

31. Hoogenboom, G.; Porter, C.H.; Boote, K.J.; Shelia, V.; Wilkens, P.W.; Singh, U.; White, J.W.; Asseng, S.; Lizaso, J.I.; Moreno, L.P.; et al. The DSSAT crop modeling ecosystem. In *Advances in Crop Modeling for a Sustainable Agriculture*; Boote, K.J., Ed.; Burleigh Dodds Science Publishing: Cambridge, UK, 2019; pp. 173–216. [CrossRef]

32. Kroes, J.G.; van Dam, J.C.; Bartholomeus, R.P.; Groenendijk, P.; Heinen, M.; Hendriks, R.F.A.; Mulder, H.M.; Supit, I.; van Walsum, P.E.V. SWAP version 4. In *Theory Description and User Manual*; University Report 2780; Wageningen Environmental Research: Wageningen, The Netherlands, 2017; p. 248. Available online: https://library.wur.nl/WebQuery/wurpubs/fulltext/416321 (accessed on 2 September 2022).

33. Westenbroek, S.M.; Engott, J.A.; Kelson, V.A.; Hunt, R.J. SWB Version 2.0—A soil-water-balance code for estimating net infiltration and other water-budget components. In *USGS Techniques and Methods 6-A59*; United States Geological Survey: Reston, VA, USA, 2018; p. 130. [CrossRef]

34. Brisson, N.; Gary, C.; Justes, E.; Roche, R.; Mary, B.; Ripoche, D.; Zimmer, D.; Sierra, J.; Bertuzzi, P.; Burger, P.; et al. An overview of the crop model STICS. *Eur. J. Agron.* **2003**, *18*, 309–332. [CrossRef]

35. Ma, L.; Ahuja, L.R.; Nolan, B.T.; Malone, R.W.; Trout, T.J.; Qi, Z. Root Zone Water Quality Model (RZWQM2): Model use, calibration and validation. *Trans. ASABE* **2012**, *55*, 1425–1446. [CrossRef]

36. Smith, M. CROPWAT: A computer program for irrigation planning and management. In *Irrigation and Drainage Paper*; Food and Agriculture Organization of the United Nations [FAO]: Rome, Italy, 1992; Volume 46, p. 128.

37. Department of Primary Industries and Regional Development (DPIRD). Soil Water Tool. 2023. Available online: https://www.agric.wa.gov.au/climate-weather/soil-water-tool/ (accessed on 13 March 2024).

38. Gaia College (GC). *Free Online Irrigation Calculator*; Gaia College: Duncan, BC, Canada, 2022; Available online: https://www.gaiacollege.ca/irrigation_calculator/Irrigation_Calculator.php (accessed on 28 August 2022).

39. Washington State University (WSU). *Irrigation in the Pacific Northwest—Irrigation Calculators*; Washington State University Extension, Oregon State University Extension, University of Idaho Extension; Washington State University: Pullman, WA, USA, 2022; Available online: http://irrigation.wsu.edu/Content/Select-Calculators.php (accessed on 28 August 2022).

40. IrrigationBox. *Irrigation Calculators*; IrrigationBox: Sumner, QLD, Australia, 2022; Available online: https://www.irrigationbox.com.au/irrigation-calculators (accessed on 28 August 2022).

41. The Partnership for Water Sustainability in British Columbia (PWSBC). Water Balance Model Online. 2023. Available online: https://waterbalance.ca/tool/water-balance-model/ (accessed on 12 March 2024).

42. Climate Smart Farming (CSF). *CSF Water Deficit Calculator*; Cornell Climate Smart Farming Program, College of Agriculture and Life Sciences, Cornell University: Ithaca, NY, USA, 2018; Available online: http://climatesmartfarming.org/tools/csf-water-deficit-calculator/ (accessed on 28 August 2022).

43. Cool Farm Alliance. *Cool Farm Tool*; Cool Farm Alliance: Lincolnshire, UK, 2019; Available online: https://coolfarmtool.org/coolfarmtool/water/ (accessed on 28 August 2022).

44. Danielescu, S. SNOSWAB (Snow, Soil Water and Water Balance Model)—A Web-Based Model. Reference Manual. 2024. Available online: https://snoswab.hydrotools.tech (accessed on 25 March 2024).

45. Office of the Chief Science Advisor of Canada [OCSAC]. *Roadmap for Open Science*; Office of the Chief Science Advisor of Canada, Government of Canada: Ottawa, ON, Canada, 2020; Available online: https://www.ic.gc.ca/eic/site/063.nsf/eng/h_97992.html (accessed on 20 October 2021).

46. Danielescu, S. Hydrology Tool Set (HTS). 2021. Available online: https://portal.hydrotools.tech (accessed on 24 March 2024).

47. Danielescu, S.; MacQuarrie, K.T.B.; Popa, A. SEPHYDRO: A Customizable Online Tool for Hydrograph Separation. *Groundwater* **2018**, *56*, 589–593. [CrossRef] [PubMed]

48. Danielescu, S.; MacQuarrie, K.T.B.; Nyiraneza, J.; Zebarth, B.; Sharifi-Mood, N.; Grimmett, M.; Main, T.; Levesque, M. Development and Validation of a Crop and Nitrate Leaching Model for Potato Cropping Systems in a Temperate–Humid Region. *Water* **2024**, *16*, 475. [CrossRef]

49. Danielescu, S. Development and Application of ETCalc, a Unique Online Tool for Estimation of Daily Evapotranspiration. *Atmos. Ocean* **2023**, *61*, 135–147. [CrossRef]

50. Danielescu, S.; MacQuarrie, K.T.B.; Zebarth, B.; Nyiraneza, J.; Grimmett, M.; Levesque, M. Crop water deficit and supplemental irrigation requirements for potato production in a temperate humid region (Prince Edward Island, Canada). *Water* **2022**, *14*, 2748. [CrossRef]

51. Danielescu, S. SWIB—An Online Model to Estimate Daily Crop Water Stress, Irrigation Needs, and Soil Water Budget. *Groundwater* **2023**, *61*, 296–300. [CrossRef] [PubMed]

52. Danielescu, S. RECHARGE BUDDY—Groundwater Recharge Estimation Tool. Reference Manual. 2024. Available online: https://rbuddy.hydrotools.tech (accessed on 25 March 2024).

53. Danielescu, S. SNOWFALL BUDDY—Snowfall and Rainfall Estimation Tool. Reference Manual. 2024. Available online: https://sbuddy.hydrotools.tech (accessed on 25 March 2024).

54. Rahgozar, M.; Shah, N.; Ross, M. Estimation of Evapotranspiration and Water Budget Components Using Concurrent Soil and Water Table Monitoring. *ISRN Soil Sci.* **2012**, *2012*, 726806. [CrossRef]

55. Ceppi, A.; Ravazzani, G.; Corbari, C.; Salerno, R.; Meucci, S.; Mancini, M. Real-time drought forecasting system for irrigation management. *Hydrol. Earth Syst. Sci.* **2014**, *18*, 3353–3366. [CrossRef]

56. Levin, S.B.; Briggs, M.A.; Foks, S.S.; Goodling, P.J.; Raffensperger, J.P.; Rosenberry, D.O.; Scholl, M.A.; Tiedeman, C.R.; Webb, R.M. Uncertainties in measuring and estimating water-budget components: Current state of the science. *WIREs Water* **2023**, *10*, e1646. [CrossRef]

57. Zebarth, B.J.; Danielescu, S.; Nyiraneza, J.; Ryan, M.C.; Jiang, Y.; Grimmett, M.; Burton, D.L. Controls on nitrate loading and implications for BMPs under intensive potato production systems in Prince Edward Island, Canada. *Groundw. Monit. Rem.* **2015**, *35*, 30–42. [CrossRef]

58. Lamb, K.; MacQuarrie, K.T.B.; Butler, K.; Danielescu, S.; Mott, E.; Grimmett, M.; Zebarth, B.J. Hydrogeophysical monitoring reveals primarily vertical movement of an applied tracer across a shallow, sloping low-permeability till interface: Implications for agricultural nitrate transport. *J. Hydrol.* **2019**, *573*, 616–630. [CrossRef]

59. Environment and Climate Change Canada (ECCC). Canadian Climate Normals for Charlottetown a Weather Station. 2021. Available online: https://climate.weather.gc.ca/climate_normals/index_e.html (accessed on 10 January 2021).

60. Bhatti, A.Z.; Farooque, A.A.; Krouglicof, N.; Peters, W.; Acharya, B.; Li, Q.; Ahsan, M.S. Spatiotemporal hydrological analysis of streamflows and groundwater recharge for sustainable water management in Prince Edward Island, Canada. *World Water Policy* **2021**, *7*, 253–282. [CrossRef]

61. Edwards, L.; Bernsdorf, B.; Pauly, M.; Burney, J.R.; Satish, M.G.; Brimacombe, M. Spatial interpolation of snow depth and water equivalent measurements in Prince Edward Island, Canada. *Can. Agric. Eng.* **1998**, *40*, 161–168. Available online: https://library.csbe-scgab.ca/docs/journal/40/40_3_161_ocr.pdf (accessed on 14 March 2023).

62. Liao, S.; Savard, M.M.; Somers, G.; Paradis, D.; Jiang, Y. Preliminary results from water isotope characterization of groundwater, surface water and precipitation in the Wilmot River Watershed, Prince Edward Island. *Geol. Surv. Can. Curr. Res. (Online)* **2005**, *5-D4*, 10. [CrossRef]

63. Carter, M.R. Physical properties of some Prince Edward Island soils in relation to their tillage requirement and suitability for direct drilling. *Can. J. Soil Sci.* **1987**, *67*, 413–487. [CrossRef]

64. Agriculture Canada Research Branch (ACRB). Soils of Prince Edward Island. In *Prince Edward Island Soil Survey*; Agriculture Canada Research Branch, Land Resource Research Centre: Ottawa, ON, Canada, 1998; p. 219.

65. Jiang, Y.; Nyiraneza, J.; Noronha, C.; Mills, A.; Murnaghan, D.; Kostic, A.; Wyand, S. Nitrate leaching and potato tuber yield response to different crop rotations. *Field. Crop. Res.* **2022**, *288*, 108700. [CrossRef]

66. Environment and Climate Change Canada (ECCC). Daily Weather Historical Data for Charlottetown a Weather Station. 2022. Available online: https://climate.weather.gc.ca/historical_data/search_historic_data_e.html (accessed on 19 April 2022).

67. National Aeronautics and Space Administration [NASA]. The Power Project. Langley Research Center (LARC). 2021. Available online: https://power.larc.nasa.gov/ (accessed on 10 March 2021).

68. National Aeronautics and Space Administration [NASA]. MODIS and VIIRS Land Products Global Subsetting and Visualization Tool. Oak Ridge National Laboratory (ORNL) Distributed Active Archive Center (DAAC). 2020. Available online: http://daacmodis.ornl.gov (accessed on 18 May 2020).

69. Cohen, J. *Statistical Power Analysis for the Behavioral Sciences*, 2nd ed.; Lawrence Erlbaum Associates: Hillsdale, NJ, USA, 1988; 567p. [CrossRef]

70. Moriasi, D.N.; Arnold, J.G.; Van Liew, M.W.; Bingner, R.L.; Harmel, R.D.; Veith, T.L. Model evaluation guidelines for systematic quantification of accuracy in watershed simulations. *Trans. ASABE* **2007**, *50*, 885–900. [CrossRef]

71. Afzaal, H.; Farooque, A.A.; Abbas, F.; Acharya, B.; Esau, T. Precision irrigation strategies for sustainable water budgeting of potato crop in Prince Edward Island. *Sustainability* **2020**, *12*, 2419. [CrossRef]

72. Jiang, Y.; Ramsay, M.; Meng, F.; Stetson, T. Characterizing potato yield responses to water supply in Atlantic Canada's humid climate using historical yield and weather data: Implications for supplemental irrigation. *Agric. Water. Manag.* **2021**, *255*, 107047. [CrossRef]

73. Francis, R. *Hydrogeology of the Winter River Basin, Prince Edward Island*; Department of the Environment: Charlottetown, PE, Canada, 1989; p. 215.

74. Paradis, D.; Vigneault, H.; Lefebvre, R.; Savard, M.M.; Ballard, J.-M.; Qian, B. Groundwater nitrate concentration evolution under climate change and agricultural adaptation scenarios: Prince Edward Island, Canada. *Earth Syst. Dynam.* **2016**, *7*, 183–202. [CrossRef]

75. MacDougall, J.I.; Veer, C. *Soils of Prince Edward Island*; LRRI Contribution No. 141; Agriculture Canada, Research Branch: Ottawa, ON, Canada, 1981; p. 141.

76. Porter, G.A.; Opena, G.B.; Bradbury, W.B.; McBurnie, J.C.; Sisson, J.A. Soil management and supplemental irrigation effects on potato: I. Soil properties, tuber yield, and quality. *Agron. J.* **1999**, *91*, 416–425. [CrossRef]

77. Wagg, C.; Hann, S.; Kupriyanovich, Y.; Li, S. Timing of short period water stress determines potato plant growth, yield and tuber quality. *Agric. Water. Manag.* **2021**, *247*, 106731. [CrossRef]

78. Jiang, Y.; Nishimura, P.; van den Heuvel, M.R.; MacQuarrie, K.T.B.; Crane, C.S.; Xing, Z.; Raymond, B.G.; Thompson, B.L. Modeling land-based nitrogen loads from groundwater-dominated agricultural watersheds to estuaries to inform nutrient reduction planning. *J. Hydrol.* **2015**, *529*, 213–230. [CrossRef]